Theor Chem Acc (2007) 118:67–73
DOI 10.1007/s00214-006-0238-6

REGULAR ARTICLE

SERS effect in CO physisorbed on homogeneous and core-shell nanoparticle aggregates

S. Bruzzone · M. Malvaldi · G. P. Arrighini ·
C. Guidotti

Received: 3 November 2006 / Accepted: 14 November 2006 / Published online: 26 January 2007

Abstract Surface Enhanced Raman Scattering (SERS) is studied for a simple molecule (CO) physisorbed on a nanoparticle belonging to a nanoparticle aggregate, with well defined composition and architecture, in order to assess the effect of metal nanostructure on the Raman enhancement. The approach involves explicit consideration of the molecule, with due allowance for the characteristics of its radiated field, which are believed to be particularly important elements in determining enhancement from complex-shape aggregates. The electrodynamic problem for a nonresonant polarizable point dipole in the presence of an aggregate of spherical scatterers has been resolved numerically, extending to a multi-particle system the treatment put forward by Kerker.

1 Introduction

Progress in SERS during the last years had open the prospect of utilizing Raman techniques for single-molecule detection (SM SERS) [1,2]. New perspectives of exploiting SERS as a sensitive analytic tool in several applications [3] (particularly in the life science context [4]) have raised the research in the field, promoting growing interest about the fundamental mechanisms involved. Despite its powerful capabilities as an analytical and diagnostic tool, the basic working mechanism of SERS is still a subject open to challenging questions. In fact, even if the fundamental effects ruling the SERS phenomenon have been recognized and their respective contributions have been often compared, an adequate theoretical framework able to lead to convincing quantitative results [5–7] is still missing.

The difficulties met in the theoretical treatment of this phenomenon are associated with the simultaneous presence of chemical (CHEM) as well as electromagnetic (EM) effects. Beyond the rigid separation between CHEM and EM effects, a correct SERS description would require to take into account for: (a) the change of the molecule properties (polarizability, radiative and nonradiative lifetime etc.) due to physisorption on the metal surface, (b) the possible (and not negligible) occurrence of new features such as charge-transfer transitions in the whole metal-molecule chemical system; (c) the modification of the electric fields (near the metal surface) driving the molecule excitation and the influence of the metal particle or aggregate of particles on the fields scattered from the molecule to the detector. Due to the overwhelming role of the electromagnetic mechanism in the SERS phenomenon, an accurate resolution of the electromagnetic scattering problem remains necessary. For this reason, many numerical studies have been performed by simply neglecting the presence of the molecule, trying to trace all experimental evidence back to the enhancement of the e.m. field on the surface of the particle [8,9]. This is clearly an approximation, which appears unsatisfactory for two main reasons. First, it neglects the importance of the modification of the scattered light frequency (Stokes shift) on the response of

---

Contribution to the Fernando Bernardi Memorial Issue.

S. Bruzzone (✉) · G. P. Arrighini · C. Guidotti
Dipartimento di Chimica e Chimica Industriale, Università degli Studi di Pisa, Via Risorgimento 35, 56126 Pisa, Italy
e-mail: sama@dcci.unipi.it

M. Malvaldi
Dipartimento di Chimica Bioorganica e Biofarmacia,
Università degli Studi di Pisa, Via Bonanno 33,
56126 Pisa, Italy

the metallic substrate (which cannot be ignorable due to the extreme sensitivity of the aggregate scattering cross section to the frequency). Second, the backscattering role from the molecule to the detector, without consideration of the molecule (and thus of the radiation source) position and polarization, is completely mistaken. We find it important to stress that even through the relative importance of all these effects to the final Raman response can be reputed a questionable point, it seems tenable that, in SM SERS, more than in traditional SERS, the role of the molecule becomes central and not ignorable with respect to the particle EM contribution [10,11].

A full, accurate treatment of both chemical and electromagnetic effects, characterized by quite different length scales, is beyond the capability of present day numerical calculations. Thus, to include all these aspects in a simulation study, a reliable and efficient separation of the chemical and the elctromagnetic problem should be developed. In fact, up to now, the largest amount of theoretical work on SERS has been focused on the chemical or the electromagnetic problem [9,11–14].

In this work, we describe a semiclassical model which, though being addressed to the solution of the electromagnetic problem, explicitly considers as a scattering source a chemically realistic model of molecule positioned near a metallic aggregate. The aggregate can be constituted of homogeneous or heterogeneous (core-shell) spherical particles. Such model locates somewhat in between the usual electromagnetic treatments often appearing in the literature [15,16] which neglect the molecule and the general quantum electrodynamic frame by Johansson, Xu and Kall [17,18] which explicitly considers the interplay between EM enhancement and vibronic molecular dynamics. Calculations similar to those we are about to present, involving homogeneous spheres and a chemically realistic molecule model in the discrete-dipole approximation, have been performed by Corni and Tomasi [19].

Our treatment neglects, in its present formulation, the modification of the properties of the molecule induced by the metal (which can be captured, in principle, according to the Johansson's suggestions [17]); such modification, however, can be included with little effort due to the general level of the description.

2 Theory

Before describing in some detail the theoretical treatment, we spend some words about the model system on which the calculations have been performed. Two kinds of particle aggregates were considered: the first one (homogeneous) consists of spherical particles of radius $R = 25\,\text{nm}$, constituted by gold or silver, while the second one (core-shell) involves spheres made of a silica core, of radius $R_{\text{core}} = 20\,\text{nm}$, coated by a metal layer (Au or Ag) of thickness $R_{\text{shell}} = 5\,\text{nm}$. The molecule retains the properties of the isolated molecule, also on the metal surface and is positioned at a distance $d = 0.5\,\text{nm}$ from the surface [21]. The incident light polarization has been kept fixed, with the electric field along the $\hat{y}$ axis and the propagation along the $\hat{x}$ axis.

2.1 Electromagnetic fields

Our treatment of the Raman scattering by a molecule absorbed at or near the surface of a spherical particle leans on ideas and methods developed elsewhere. The first mention is reserved to Kerker and coworkers [22], who provided a physically sound model for Raman scattering by a molecule absorbed at the surface of a spherical particle, with the molecule treated as a classical electric dipole. The second one is a recognition to Gerardy and Ausloos [23] work, for their contribution to the study of optical properties of aggregated metal spheres taking into account the electromagnetic coupling among all particles. This means that the following description is a theory general enough to include magnetic multipolar orders and their coupling to the electric multipoles.

The whole e.m. scattering process near a surface can be viewed in two steps. In the first one, the molecule (located at $\vec{r}'$) behaves like a dipole $\overrightarrow{p}$ stimulated by a local primary field $\overrightarrow{E}_{\text{p}}\left(\vec{r}';\omega_0\right)$, comprising the incident $\overrightarrow{E}_{\text{i}}\left(\vec{r}';\omega_0\right)$ and the Lorenz–Mie scattered field $\overrightarrow{E}_{\text{LM}}$ $\left(\vec{r}';\omega_0\right)$ at frequency ω_0, so that:

$$\vec{p} = \alpha \cdot \vec{E}_{\text{p}}\left(\vec{r}';\omega_0\right) = \alpha \cdot \left[\vec{E}_{\text{i}}\left(\vec{r}';\omega_0\right) + \vec{E}_{\text{LM}}\left(\vec{r}';\omega_0\right)\right], \quad (1)$$

where α denotes the molecular Raman polarizability tensor. The involved fields $\overrightarrow{E}_{\text{i}}\left(\vec{r}';\omega_0\right)$ and $\overrightarrow{E}_{\text{LM}}\left(\vec{r}';\omega_0\right)$ can be expanded in terms of spherical vector harmonics,

$$\vec{E}_{\text{i}}\left(\vec{r}',\omega_0\right) = \sum_{\nu}\left[f_\nu(j)\,\vec{M}_\nu^{\prime 1,j}\left(k_0\vec{r}'\right) + g_\nu(j)\,\vec{N}_\nu^{\prime 1,j}\left(k_0\vec{r}'\right)\right] \quad (2)$$

$$\vec{E}_{\text{LM}}\left(\vec{r}',\omega_0\right)\sum_{\nu}\left[a_\nu(j)\,\vec{M}_\nu^{\prime 3,j}\left(k_0\vec{r}'\right) + b_\nu(j)\,\vec{N}_\nu^{\prime 3,j}\left(k_0\vec{r}'\right)\right]$$
$$+\sum_{\mu}\sum_{i\neq j}^{N}\left[a_\mu(i)\,\vec{M}_\mu^{\prime 3,k}\left(k_0\vec{r}'\right) + b_\mu(i)\,\vec{N}_\mu^{\prime 3,k}\left(k_0\vec{r}'\right)\right] \quad (3)$$

with k_0 the real wavenumber, referred to the incident frequency, in the matrix embedding the whole system and $\sum_\nu = \sum_{n=1}^{\infty}\sum_{m=-n}^{n} \cdot \vec{M}_\nu^{\prime 3,j}\left(k_0\vec{r}\right)$ and $\vec{N}_\nu^{\prime 3,j}\left(k_0\vec{r}\right)$ are spherical vector harmonics, defined in the frame centered on the jth sphere, with the superscript 3 (or 1) indicating an outgoing (incoming) spherical wave. The Maxwell's boundary conditions, for the electric and magnetic fields at each particle surface, lead to linear equations sets for the expansion coefficients $a_\nu(i)$ and $b_\nu(i)$ of the scattered wave. Obviously, the incident wave coefficients $f_\nu(i)$ and $g_\nu(i)$ referred to each particle i involved in the system are known, once polarization of the incident field and aggregate topology are defined. (For a more exhaustive explication, the reader is referred to the original works [22,23]). For our purposes, the interest can be limited to the fields at the surface and outside the particles; then, for core-shell particles, the equation set can be solved more quickly by embedding the effect of morphology and architecture of the particle directly into the scattering coefficients [24,25].

The second step of the process correspond to the emission of radiation by the active molecule, at the shifted frequency ω. In addition to the radiated dipole field, $\vec{E}_{\text{dip}}(\vec{r},\omega)$:

$$\vec{E}_{\text{dip}}(\vec{r},\omega) = \begin{cases} \sum_\nu \left[s_\nu(j)\,\vec{M}_\nu^{3,j}(k\vec{r}) + t_\nu(j)\,\vec{N}_\nu^{3,j}(k\vec{r}) \right], & r > r' \\ \sum_\nu \left[p_\nu(j)\,\vec{M}_\nu^{1,j}(k\vec{r}) + q_\nu(j)\,\vec{N}_\nu^{1,j}(k\vec{r}) \right], & r < r' \end{cases} \tag{4}$$

a secondary, scattered field is involved, that must be obtained by satisfying the proper boundary conditions at the surfaces of the particles,

$$\vec{E}_{\text{sc}}(\vec{r},\omega) = \sum_\nu \left[u_\nu(j)\,\vec{M}_\nu^{3,j}(k\vec{r}) + v_\nu(j)\,\vec{N}_\nu^{3,j}(k\vec{r}) \right] + \sum_{i\neq j}^{N} \sum_\mu \left[u_\mu(k)\vec{M}_\mu^{3,i}(k\vec{r}) + v_\mu(k)\vec{N}_\mu^{3,i}(k\vec{r}) \right] \tag{5}$$

As $\vec{E}_{\text{LM}}(\vec{r}';\omega_0)$, even $\vec{E}_{\text{sc}}(\vec{r};\omega)$ is a sensitive function of particle aggregate topology, dimension, structure and optical properties of the single particles, as well as of the frequency and polarization of the dipole field.

As previously discussed, the solution of the electromagnetic problem consists of obtaining the correct coefficients for the field expansion (Eq. 5) by applying the appropriate boundary conditions in order to evaluate all the electric fields in any location. Following the same treatment based on the boundary condition at the surface of particles, which gives the coefficients $a_\nu(i)$ and $b_\nu(i)$ of Eq. 3, two sets of linear equation have to be handled. The problem is analogous to that treated previously in the first step, with the difference that the coefficients related to the incident wave, $f_\nu(i)$ and $g_\nu(i)$, must be replaced by $p_\nu(i)$ and $q_\nu(i)$, whose meaning is evident from Eq. 4 (the analytical expressions are reported by Kerker [22]).

The Raman enhancement can be evaluated as the ratio between the total field at the shifted frequency ω for whole system and $\vec{E}_{\text{dip}}^{\text{alone}}(\vec{r}';\omega)$, the field that would have been scattered by the stand-alone molecule:

$$\eta = \frac{\left| \vec{E}_{\text{dip}}(\vec{r}',\omega) + \vec{E}_{\text{sc}}(\vec{r}',\omega) \right|^2}{\left| \vec{E}_{\text{dip}}^{\text{alone}}(\vec{r}',\omega) \right|^2} \tag{6}$$

Instead of evaluating the fields in correspondence of the detector, assumed to be placed at long distance from the scattering system, the enhancement has been tested at the molecule position $\vec{r}'$. Estimates of the Raman enhancement caused by EM effects are frequently based on the electric field $\vec{E}_{\text{p}}(\vec{r}',\omega_0) = \vec{E}_{\text{in}}(\vec{r}',\omega_0) + \vec{E}_{\text{LM}}(\vec{r}',\omega_0)$, as obtained from the first step of the scattering process, ignoring in conclusion the presence of the molecule and its role [21,26]. Although approximate, our treatment seems to capture features closer to the actual physical situation.

The scattering cross section is an alternative optical property frequently employed to estimate electromagnetic interactions among clusters and, indirectly, the electric fields $\vec{E}_{\text{p}}(\omega_0)$ involved in the scattering processes [27]. Following Quinten and Kreibig [24], in terms of the previous notation, the scattering cross section for an aggregate of N nanoparticles is evaluated by:

$$C_{\text{sca}} = \frac{2\pi}{k_0^2} \sum_{i=1}^{N} \sum_{n=1}^{\infty} \sum_{m=.n}^{n} |a_{nm}(i)|^2 + |b_{nm}(i)|^2 + \frac{2\pi}{k_0^2} \sum_{i=1}^{N} \sum_{n=1}^{\infty} \sum_{m=.n}^{n} \text{Re}\left\{ a_{nm}(i)\left(1 - \frac{a_{nm}(i)}{\Gamma_n(i)}\right) + b_{nm}(i)\left(1 - \frac{b_{nm}(i)}{\Delta_n(i)}\right) \right\} \tag{7}$$

where $\Gamma_n(i)$ and $\Delta_n(i)$ are the scattering coefficients of the single isolated sphere i for the n order TM and TE modes, respectively, as follows from the Mie's theory [25].

2.2 Particle dielectric function

The permittivity of the silica core is considered independent of the frequency and equal to the silica bulk value (2.56), whereas that of the metal nanostructures considered in this paper is calculated according to a semiempirical oversimplified model, widely utilized [28–30], based on the Drude theory [31] and experimental

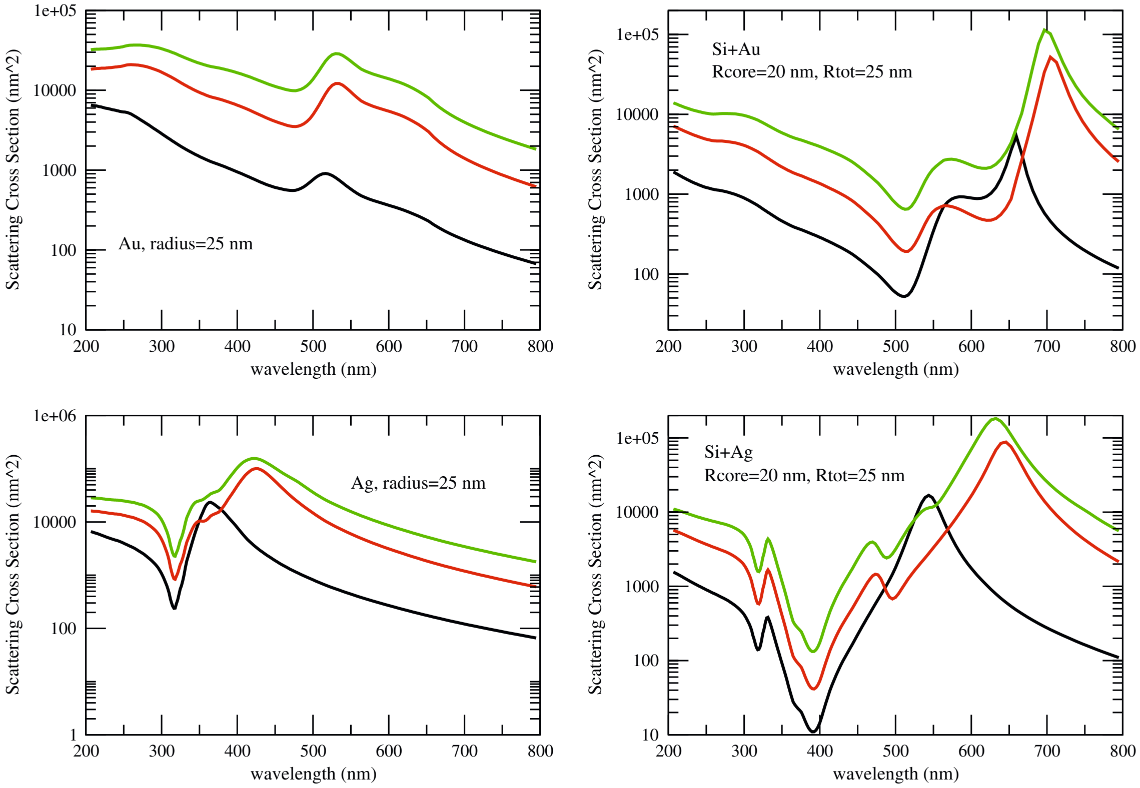

Fig. 1 Scattering cross section versus incident wavelength λ_0 for 1 (*black line*), 2 (*red line*) and 4 (*green line*) particles (see Fig. 2 for system geometric details). Particles are constituted by Au (*top left*), Ag (*bottom left*), Si core + Au shell (*top right*) and Si core + Ag shell (*bottom right*)

dielectric bulk data. For the case of a pure metal homogeneous particle or for the metal shell of a silica nanoshell, the dielectric function can be explicited as follows:

$$\begin{aligned}\varepsilon(\omega,R) &= \varepsilon_{\text{exp}}(\omega) - \varepsilon^{\text{Drude}}_{\text{bulk}}(\omega) + \varepsilon^{\text{Drude}}_{\text{nanostructure}}(\omega,R)\\ &= \varepsilon_{\text{exp}}(\omega) + \frac{\omega_p^2}{\omega^2 + i\omega\Gamma_\infty}\\ &\quad - \frac{\omega_p^2}{\omega^2 + i\omega(\Gamma_\infty + \Gamma_{\text{nanostructure}})}\end{aligned} \tag{8}$$

where $\varepsilon_{\text{exp}}(\omega)$ is the experimental permittivity of the pure bulk material [32], ω_p the plasma frequency ($1.372 \times 10^{16}\,\text{s}^{-1}$ for Au and $1.365 \times 10^{16}\,\text{s}^{-1}$ for Ag) and $\Gamma_\infty = v_F/l_\infty$ the bulk electron collision frequency, ratio between the Fermi velocity v_F and the mean free path l_∞ of the conduction electrons in the metal bulk. $\Gamma_{\text{nanostructure}}$ is the surface-induced contribution to the damping, a quantity depending on the nature of the system. Generally speaking, $\Gamma_{\text{nanostructure}} = A_{\text{nanostructure}} v_F / l_{\text{nanostructure}}$, with $l_{\text{nanostructure}}$ and $A_{\text{nanostructure}}$ characteristic parameters of the geometry of the system. The values of $l_{\text{nanostructure}}$ for a perfect metal shell or for a homogeneous pure metal spherical particle are set equal to the thickness of the shell R_{shell} or the total radius particle R_{tot}, respectively. $A_{\text{nanostructure}}$ is a proper parameter describing the loss of coherence by scattering events. While there is plenty of literature providing estimates of $A_{\text{nanostructure}}$ for a homogeneous metal spherical particle, a reasonable estimate of the same parameter in our case is not straightforward to infer. In this work, the values used are $A_{\text{core}} = 1$ and $A_{\text{shell}} = 0.5$ [29].

2.3 Molecule

The chosen molecule (carbon monoxide, CO) is a simple substrate well studied for its Raman and SERS properties. In this paper we have limited our study to the first Stokes vibronic line (2,111 cm^{-1}, corresponding to a frequency shift 0.009621 a.u.).

The molecule has been treated as a polarizable dipole; because of the strength of the fields acting at the metal surface, the molecule is supposed to be perfectly aligned with the driving field [33,34].

This allows us to reduce the polarizability tensor to a single diagonal term and to solve the quantum-mechanical problem for the molecule in its monodimensional form in the spirit of the Born-Oppenheimer approximation. The vibrational eigenstates and vibronic dipole moments have been calculated starting from electronic states taken from literature [35].

The Raman dynamic polarizability of the system, as known, can be expressed in the form:

$$\alpha_{zz}\left(-\omega_0;\omega\right) = \sum_r \sum_{\upsilon''} \left\{ \frac{\left\langle \chi_{0\upsilon'} \left| \left\langle \varphi_0 \left| \mu_z \right| \varphi_r \right\rangle \right| \chi_{r\upsilon''} \right\rangle \left\langle \chi_{r\upsilon''} \left| \left\langle \varphi_r \left| \mu_z \right| \varphi_0 \right\rangle \right| \chi_{00} \right\rangle}{E_{r0} + \varepsilon_{r\upsilon'',00} - \hbar\omega_0} + \frac{\left\langle \chi_{0\upsilon'} \left| \left\langle \varphi_0 \left| \mu_z \right| \varphi_r \right\rangle \right| \chi_{r\upsilon''} \right\rangle \left\langle \chi_{r\upsilon''} \left| \left\langle \varphi_r \left| \mu_z \right| \varphi_0 \right\rangle \right| \chi_{00} \right\rangle}{E_{r0} + \varepsilon_{r\upsilon'',00} + \hbar\omega} \right\} \quad (9)$$

where $\varphi_r, \chi_{0\upsilon'}$ denote electronic and vibrational functions, respectively, $E_{ro}, \varepsilon_{rv'',00}$ being the proper energy differences involved.

3 Results

As expected, the electromagnetic coupling between the particles leads to modification of the resonance plasmon of the metal aggregate with respect to the one of a single particle, strongly dependent on the geometry of the aggregate. Our first aim is then to quantify the role of such interactions for aggregates consisting of both homogeneous and core-shell entities. The coupling importance can be assessed by inspection of Fig. 1, where calculated scattering cross sections (C_{sca}), for a single particle, a couple and an array of four particles are reported as a function of the incident wavelength (see Fig. 2 for the geometric references). The main effects of the coupling are seen to be a red-shift of the scattering maximum, along with enhancement of the absolute value of the scattering cross section. Such enhancement is sizeable (about one order of magnitude) when passing from a single particle to a dimer, whereas it is appreciably smaller, even if still evident, as we move from the dimer to the four-particle array. The smaller change resulting in the latter case may be attributed to the particular geometry of the aggregates as well as to the orientation of the field chosen, but is observed independently of the internal geometry of the single nanoparticles. The same remarks, in fact, hold for both homogeneous and core-shell systems.

At the same time, the e.m. coupling modifies the near-field response and can give rise, in particular, to limited zones where the electric field modulus is greatly augmented (hot-spots), a hint that there the factor η is expected to be strongly affected by the presence of interparticle e.m. coupling. An immediate confirmation of this remark is deducible from the inspection of Fig. 3, where the behavior of the Raman enhancement is plotted versus the wavelength of the scattered radiation.

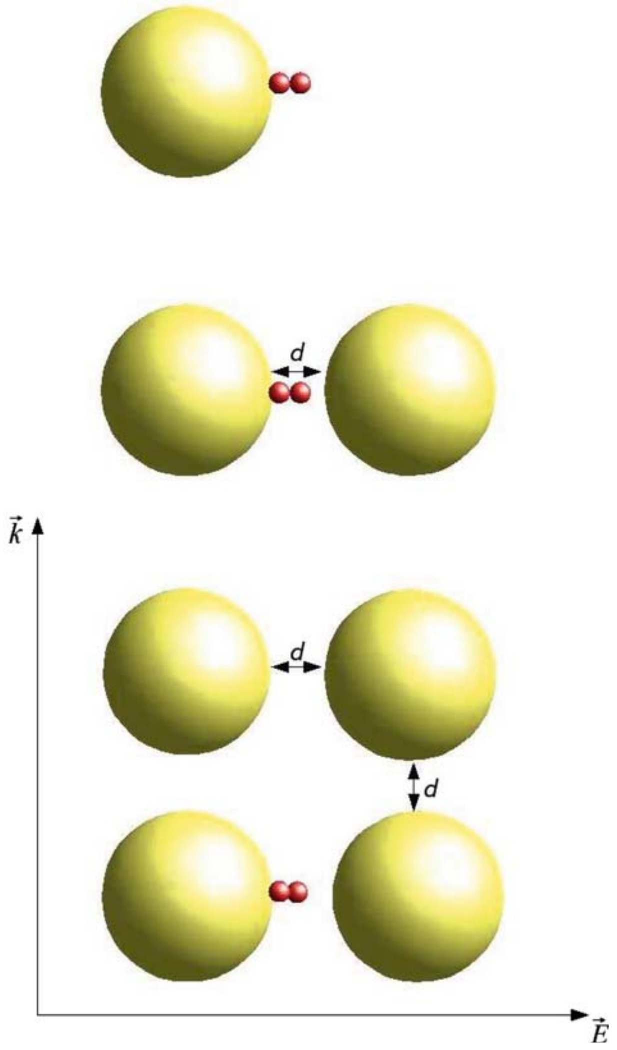

Fig. 2 Pictorial setup of the systems studied in Figs. 1 and 3. The *red cylinder* represents the molecule position and alignment in space

Similarly to what is observed for the scattering cross-section (and not surprisingly) the formation of an aggregate pushes up the enhancement to a noticeable extent but, contrarily to the behavior of the scattering cross section, the SERS enhancements for aggregates involving more than one particle, are comparable,at least for the geometries investigated. The question, however, probably deserves further analysis.

We must recall that while C_{sca} is a property of the metal aggregate in the absence of the molecule, in the calculation of the SERS enhancement the molecule with its frequency-dependent polarizability and position on the aggregate surface is explicitly considered. The two response properties sample two inherently different systems: C_{sca}, by definition, involves an integration over the whole solid angle, while the SERS enhancement is performed in a precise local point.

Table 1 Wavelength of maximum of Raman scattering enhancement η and wavelength of maximum of scattering cross-section C_{sca} for each system studied

	Wavelength of maximum of Raman scattering enhancement		Wavelength of maximum of scattering cross-section
Number and kind of particles	Incident field, λ_0(nm)	Raman scattered field, λ(nm)	Incident field, λ_0(nm)
Au 1	525.3	590.9	516.6
Au 2	534.4	602.4	529.8
Au 4	543.8	614.3	529.8
Ag 1	364.7	395	364.6
Ag 2	424.6	466.4	424.6
Ag 4	427.5	469.9	421.7
Si + Au 1	659.5	766.2	659.5
Si + Au 2	704.5	827.6	704.5
Si + Au 4	696.5	816.6	696.5
Si + Ag 1	543.8	614.3	543.8
Si + Ag 2	645.7	647.7	645.7
Si + Ag 4	632.6	730	632.6

λ_0 and λ are referred to the incident light and Raman scattered light, respectively

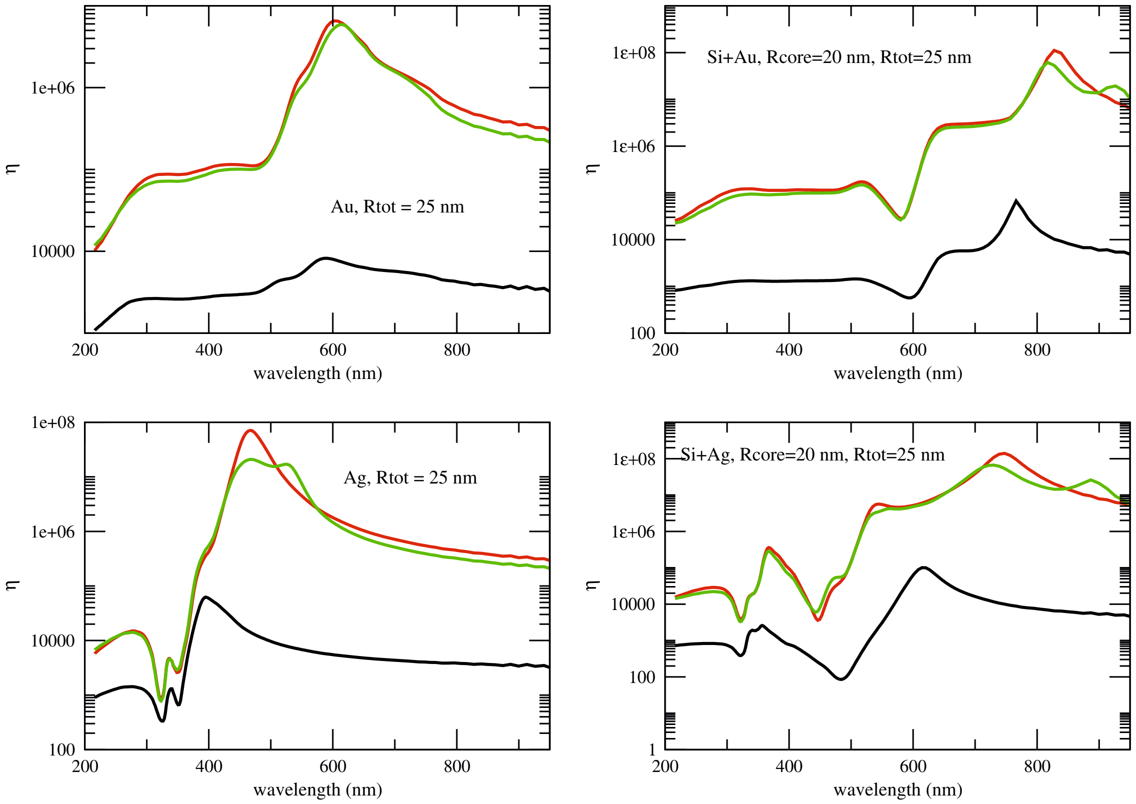

Fig. 3 Raman enhancement factors η calculated according to Eq. 6 versus scattered wavelength λ for 1 (*black line*), 2 (*red line*) and 4 (*green line*) particles (see Fig. 2 for system geometric details). Particles are constituted by Au (*top left*), Ag (*bottom left*), Si core + Au shell (*top right*) and Si core + Ag shell (*bottom right*)

An aspect to be noted is the correlation between the position of the enhancement maximum (which is to be compared with the incident light wavelength) and that of the scattering cross section. To facilitate this comparison, we collect in Table 1 the respective maxima along with the corresponding values of the incident light wavelength. It is immediately clear that η and C_{sca} display the maximum value almost at the same wavelength of the incident field, an occurrence particularly evident for core-shell systems. These findings can be explained invoking the role of the electron surface plasmon of the particles. Indeed, both the two properties studied, as a consequence of the electron plasmons, exhibit their maxima in correspondence of the plasmon resonance wavelength.

4 Conclusion

In this work, we have developed a semiclassical model to study the e.m. SERS effect provided by a single molecule adsorbed on the surface of an aggregate of spherical metal particles. Our study was focused on the influence of collective plasmons (or, in other words, of the electromagnetic coupling between particles) on the SERS phenomenon. In an ideal continuation, it is reasonable to expect a ready extension of the treatment to an ensemble of molecules covering the particles, so as to mimick more realistic experimental situations.

The formation of an aggregate (as simply as a dimer) unconditionally raises the electromagnetic enhancement; this effect is equally intense for simple metal and core-shell particle. We can underline two significant aspects emerging through the comparison of the response obtained from the two optical properties studied, C_{sca} and η. The different nature of these two properties becomes evident taking into account the response of the involving two and four particles aggregates here considered. C_{sca} gets larger as the number of particle increases, while η remains almost unchanged.

It seems also noticeable the coincidence, at the incident frequency level, of the core-shell scattering cross section and enhancement factor maxima. It means that the most intense SERS response is obtained with a frequency of the incident field corresponding to the plasmon resonance, determined by the e.m. coupling between the particles, while the molecule role is only limited to determine the shift frequency amount.

Acknowledgments This study was supported by the Italian MIUR, Ministero dell'Istruzione, Università e Ricerca (FIRB 2001: "Optical properties of molecular systems at interphases" and PRIN 2005: "Trasferimenti di energia e di carica a livello molecolare").

References

1. Nie S, Emory SR (1997) Science 275:1102
2. Michaels AM, Nirmal M, Brus LE (1999) J Am Chem Soc 121:9932
3. Dieringer JA, McFarland AD, Shah NC, Stuart DA, Whitney AV, Yonzon MA, Zhang XY, Van Duyne RP (2006) Faraday Discus 132:9
4. Chowdhury MH, Gant VA, Trache A, Baldwin A, Meininger GA, Cote GL (2006) J Biomed Optics 11:24004
5. Jensen J, Zhao LL, Autschbach J, Schatz GC (2005) J Chem Phys 123:174110
6. Pustovit VN, Shahbazyan TV (2006) Phys Rev B 73:085408
7. Arenas JF, Soto J, Tocòn IL, Fernandez DJ, Otero JC, Marcos JI (2002) J Chem Phys 116:7207
8. Schatz GC, Van Duyne R (2002) Electromagnetic mechanism of surface enhanced spectroscopy. In: Chalmers JM, Griffiths PR (eds) Handbook of vibrational spectroscopy, vol 1. Wiley, New York
9. Etchegoin P, Cohen LF, Hartigan H, Brown RJC, Milton MJT, Gallop JC (2003) J Chem Phys 119:5281
10. Zhao L, Jensen L, Schatz GC (2006) J Am Chem Soc 128:2911
11. Gibson JW, Johnson BR (2006) J Chem Phys 124:064701
12. Oubre C, Nordlander P (2005) J Phys Chem B 109:10042
13. Zhao X, Fang Y (2006) J Mol Struct 789:157
14. Wu DY, Hayashi M, Lin SH, Tian ZQ (2004) Spectrochim Acta (Part A) 60:137
15. Corni S, Tomasi J (2001) J Chem Phys 114:3739
16. Jackson JB, Westcott SL, Hirsch LR, West JL, Halas NJ (2003) App Phys Lett 82:257
17. Jackson JB, Halas NJ (2004) PNAS 101:17930
18. Xu H, Wang X-H, Persson MP, Xu HQ, Kall M, Johansson P (2004) Phys Rev Lett 93:243002
19. Johansson P, Xu H, Kall M (2005) Phys Rev B 72:035427
20. Corni S, Tomasi J (2002) J Chem Phys 116:1156
21. Zhao K, Hongxing X, Baohua G, Zhenyu Z (2006) J Chem Phys 125:081102
22. Kerker M, Wang D-S, Chew H (1980) App Opt 19:4159
23. Gérardy JM, Ausloos M (1982) Phys Rev B 25:4204
24. Quinten M, Kreibig U (1993) App Opt 32:6173
25. Bohren CF, Huffman DR (1983) Absorption and scattering of light by small particles. Wiley, New York
26. Talley CE, Jackson JB, Oubre C, Grady NK, Hollars CW, Lane SM, Huser TR, Nordlander P, Halas NJ (2005) Nano Lett 5:1569
27. Quinten M (1998) Appl Phys B 67:101
28. Euler J (1954) Z Phys 137:318
29. Bruzzone S, Malvaldi M, Arrighini GP, Guidotti C (2006) J Phys Chem B 110:11050
30. Averitt RD, Sarkar D, Halas NJ (1997) Phys Rev Lett 78:4217
31. Kreibig U, Vollmer M (1995) Optical properties of metal clusters, Springer, Berlin
32. Palik ED (1985) Handbook of optical constants of Solids, vol 1. Academic, Orlando
33. Van Leuven P, Malvaldi M, Persico M (2002) J Chem Phys 116:538
34. Seideman T (1997) J Chem Phys 106:2881
35. Cooper DM, Langhoff SR (1981) J Chem Phys 74:1200